

Impact of Spatial Variations on Splitter-Tree-Based Integrated Optical Phased Arrays

Zhengxing Zhang,^{1,*} Milica Notaros,² Zhengqi Gao,¹ Uttara Chakraborty,¹
Jelena Notaros,² and Duane S. Boning¹

¹Microsystems Technology Laboratories, Massachusetts Institute of Technology, Cambridge, MA 02139, USA

²Research Laboratory of Electronics, Massachusetts Institute of Technology, Cambridge, MA 02139, USA

*zhxzhang@mit.edu

Abstract: We consider the impact of spatially correlated geometric variations on splitter-tree-based integrated optical phased arrays. These variations can substantially affect the emitted beam. Our analysis is shown to be consistent with experimental results. © 2023 The Author(s)

1. Introduction

Several studies [1–4] in recent years have explored manufacturing process variations and their impact on integrated photonics, for the goal of achieving high yield and performance of photonic circuits. However, while a relatively wide range of process variation types have been covered, most of the studies are still limited to single photonic components or small-scale photonic circuits.

Integrated optical phased arrays (OPAs) are an emerging class of photonic systems that enable manipulation and dynamic control of free-space light in a compact form factor, at low costs, and in a non-mechanical way [5–9]. However, as large-scale photonic circuits spanning across millimeters and consisting of hundreds or thousands of device components, these integrated phased arrays can be highly susceptible to various types of process variations. It is desirable to study the impact of process variations on phased arrays so that we can obtain more robust designs that achieve high performance given actual manufacturing limitations.

In this work, we study the impact of spatial variation – specifically, the variations in waveguide thickness or width across the wafer arising from deposition and etching processes. We aim to identify the behavior and mechanism by which these spatial variations affect the shape of the beam emitted from the phased array. Specifically, we focus on phased arrays based on a splitter-tree architecture [8, 9].

2. Splitter-Tree Architecture and Sources of Variation

As shown in Fig. 1(a), a splitter-tree-based phased array consists of a splitter-tree structure that distributes input power equally to each antenna row, phase modulators that control the beam steering, and antenna rows with periodic perturbations [8, 9]. Here, we focus on the case with no active beam steering, and ignore the effect from phase modulators. The potential impact of fabrication variations can be broken into four components: phase variation at the waveguides of the splitter-tree structure, amplitude imbalance of the splitters, phase variation at the antennas, and amplitude variation along the antenna perturbations.

The spatial variation due to fabrication variations can be modeled as zero-mean spatially correlated random Gaussian noise with covariance $\text{cov}[\zeta(x, y), \zeta(x', y')] = A^2 \exp\left[-\frac{(x-x')^2 + (y-y')^2}{L_c^2}\right]$, where $\zeta(x, y)$ is the thickness or width variation at location (x, y) , and amplitude A and correlation length L_c are the parameters that control the magnitude and length scale of the Gaussian noise. Typically, L_c is much longer than the length scale of the phased array [3]; therefore, the distribution of the variation can be approximated as $\zeta(x, y) = g_x x + g_y y + \zeta_0$, with $g_x, g_y \sim \mathcal{N}(0, A^2/2L_c^2)$ being normally distributed random variables representing the gradient of the geometric variation (thickness or width) in the two dimensions. For spatial variation with very long correlation length, simulation results show that the amplitude imbalance of the splitters and the amplitude variation at the antenna perturbations are both insignificant compared to the effect of phase variation. Therefore, we only focus on the phase variation in our analysis.

We start by simulating the phase variation and the resulting beam shape of a silicon phased array having nine sequential splitter layers, 512 antennas, an antenna pitch of 2 μm , and a design wavelength of 1550 nm, and consider different values of g_x and g_y in the waveguide width variation. For the visualization, we center the beam shape at the peak of the mainlobe, and normalize the angles separately along the two dimensions so that the width of the mainlobe is the same along the array and antenna dimensions. When variation along the x -axis is applied (g_x), no significant impact on the emitted beam pattern is observed, as shown in Fig. 1(b). On the other hand,

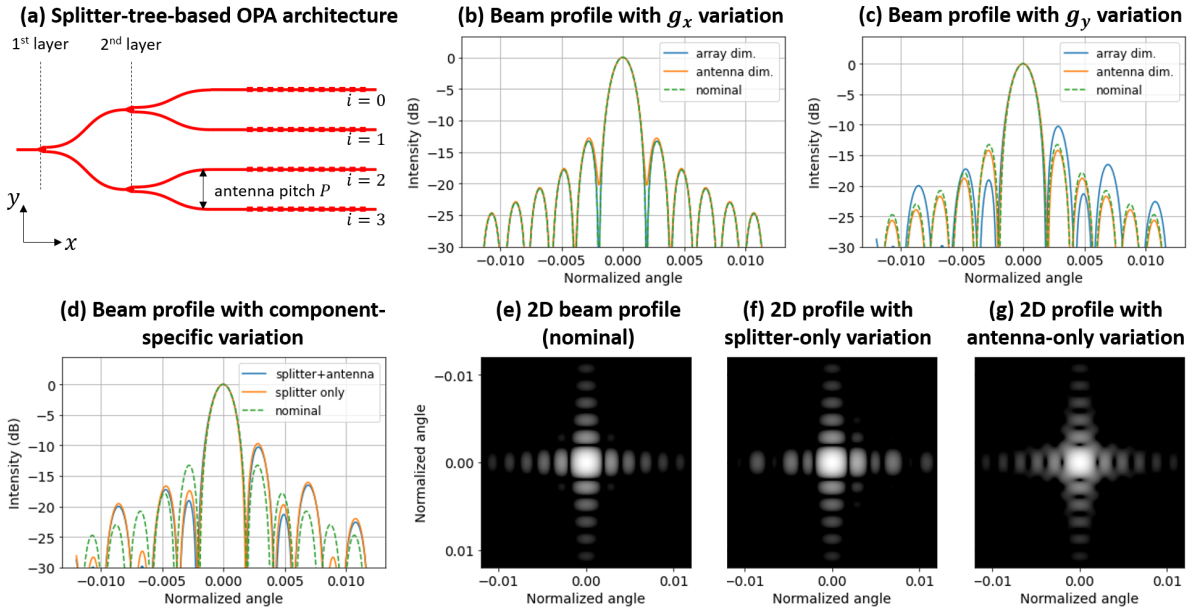


Fig. 1. (a) Simplified top-view schematic of a splitter-tree-based phased array with two splitter layers. The emitted beam shape in the array dimension (blue) and antenna dimension (orange) when applying a width variation spatial gradient of 0.5 nm/mm along the (b) x -axis and (c) y -axis. (d) The emitted beam shape along the array dimension when applying variation to both the splitter tree and the antennas (blue) versus only the splitter tree (orange). The 2D intensity distribution of the emitted beam (e) of the nominal case, when applying the variation to (f) only the splitter tree and (g) only the antennas. (d,f-g) apply the same variation as in (c).

when variation along the y -axis is applied (g_y), the emitted beam pattern in the array dimension is significantly impacted; there is an increase in the sidelobe level (SLL) on one side of the mainlobe, as shown in Fig. 1(c).

We can also separate the effect due to variations in the splitter-tree section versus variations along the antennas by applying the spatial variation only to certain parts of the phased array structure. As shown in Fig. 1(d), the variation in the splitter-tree structure dominates the impact on the beam shape along the array dimension. However, the effect of the variation along the antenna rows cannot be ignored when looking at the 2D distribution of the beam profile, as shown in Fig. 1(e-g).

3. Phase Variation Pattern Due to Thickness and Width Variations

Since we identified that the dominant sensitivity is due to the phase change in the splitter-tree structure, we can describe the effect of the spatial variation by the phase variations p_i at the beginning of each antenna row i (shown in Fig 1(a)). We can show that $p_i = g_y f_i + C_1 i + C_0$, where the phase variation pattern f_i only depends on the design of the splitter tree, the type of variation (thickness or width), and the material. The additional linear term $C_1 i + C_0$ can only change the location of the lobes; thus the pattern f_i determines the effect on the beam shape.

We show in Fig. 2(a) the phase variation pattern f_i for the thickness and width variation on a silicon phased array with nine splitter layers and an antenna pitch of 2 μm . Notably, the pattern has the same behavior for thickness and width variation, with a difference of approximately just a scaling factor. This is because the pattern is dominated by the phase change of the routing waveguides with identical specifications, and different types of geometric variation all affect the phase by perturbing the effective index of the waveguide mode.

With these discussions, it is sufficient that we only focus on the analysis of one type of variation (e.g., the thickness variation) in the following discussion, since the other types will only differ by a scaling factor.

4. Effect of the Splitter-Tree Architecture Parameters on Variations

The phase variation pattern f_i shown in Fig. 2(a) is dominated by the sharp jump at the center, which is the phase difference between the middle two antenna rows. This phase jump is also the dominant factor for the increase in SLL. Intuitively, splitter trees with more layers (and hence longer paths) or larger antenna pitch (and hence greater difference in variation) will increase this phase jump, and thus result in a larger impact on SLL. This is validated by the simulation results of various phased array designs with different numbers of splitter layers (L) and antenna pitches (P), as shown in Fig. 2(b).

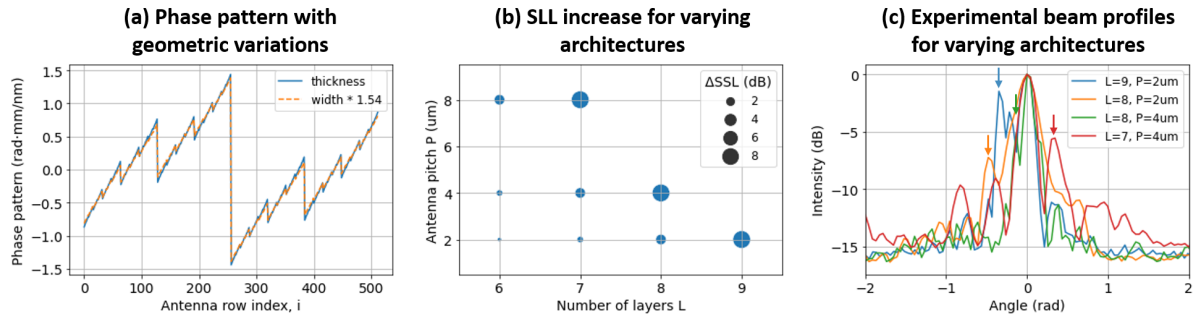


Fig. 2. (a) The phase variation pattern f_i of the thickness (blue) and width (orange, scaled) variation on the example phased array. (b) The predicted increase in sidelobe level (SLL) of different splitter-tree architectures when applying thickness variation gradient of $g_y = 1$ nm/mm. (c) Experimentally measured data of phased arrays with various architecture properties showing the emitted beam intensity along the array dimension.

5. Validation through Experimental Results

Next, we validate our theoretical findings by experimentally measuring the output far-field beam profiles for multiple splitter-tree-based integrated optical phased arrays. The phased arrays were fabricated in a CMOS-compatible 300-mm wafer-scale silicon-photonics process at the State University of New York Polytechnic Institute's (SUNY Poly) Albany NanoTech Complex [8, 9].

Experimental results showing the emitted far-field beam profiles for phased arrays with different numbers of layers and antenna pitches are shown in Fig. 2(c). As expected, the emitted patterns have asymmetric sidelobes and an increase in SLL with respect to the nominal simulated case. Notably, the increase in SLL with respect to layer number and antenna pitch roughly follows the same trend as shown in our variation simulations. However, compared to the simulation results where the sidelobe on one side of the main lobe is always lower than the nominal value, we observe that the sidelobe peaks are higher than the nominal value on both sides in the measurement result, which indicates the impact of other process variations (e.g., a pattern density effect).

6. Conclusions

We evaluate the impact of spatial waveguide geometric variations on splitter-tree-based integrated optical phased arrays, and show that such variations cause increased sidelobe levels along the array dimension primarily by affecting the phase distributions in the splitter tree. We show how varying the number of splitter layers and antenna pitch affects the sidelobe suppression, and confirm these theoretical findings by observing a similar trend in actual experimental measurements. These results can be used as a guideline for phased array designs in the future, and the phase variation pattern f_i can be useful for fast calibration of active phased arrays.

References

1. D. Melati, A. Melloni, and F. Morichetti, "Real photonic waveguides: guiding light through imperfections," *Advances in Optics and Photonics*, vol. 6, no. 2, pp. 156–224, 2014.
2. S. I. El-Henawy, R. Miller, and D. S. Boning, "Effects of a random process variation on the transfer characteristics of a fundamental photonic integrated circuit component," in *Optical Modeling and Performance Predictions X*, vol. 10743. International Society for Optics and Photonics, 2018, p. 107430O.
3. Y. Xing, J. Dong, S. Dwivedi, U. Khan, and W. Bogaerts, "Accurate extraction of fabricated geometry using optical measurement," *Photonics Research*, vol. Mar, no. 11, pp. 1008–1020, 2018.
4. Y. Xing, J. Dong, U. Khan, and W. Bogaerts, "Correlation between pattern density and linewidth variation in silicon photonics waveguides," *Optics Express*, vol. 28, no. 6, pp. 7961–7968, 2020.
5. J. Sun, E. Timurdogan, A. Yaacobi, E. S. Hosseini, and M. R. Watts, "Large-scale nanophotonic phased array," *Nature*, vol. 493, pp. 195–199, 2013.
6. F. Aflatouni, B. Abiri, A. Rekhi, and A. Hajimiri, "Nanophotonic projection system," *Optics Express*, vol. 23, no. 16, pp. 21 012–21 022, 2015.
7. J. Doyle, M. Heck, J. Bovington, J. Peters, L. Coldren, and J. Bowers, "Two-dimensional free-space beam steering with an optical phased array on silicon-on-insulator," *Optics Express*, vol. 19, no. 22, pp. 21 595–21 604, 2011.
8. C. V. Poulton, M. J. Byrd, M. Raval, Z. Su, N. Li, E. Timurdogan, D. Coolbaugh, D. Vermeulen, and M. R. Watts, "Large-scale silicon nitride nanophotonic phased arrays at infrared and visible wavelengths," *Optics Letters*, vol. 42, no. 1, pp. 21–24, 2017.
9. J. Notaros, C. V. Poulton, M. Raval, and M. R. Watts, "Near-field-focusing integrated optical phased arrays," *Journal of Lightwave Technology*, vol. 36, no. 24, pp. 5912–5920, 2018.